Agenzia Nazionale per le Nuove Tecnologie,
l'Energia e lo Sviluppo Economico Sostenibile

Ministero dello Sviluppo Economico

RICERCA DI SISTEMA ELETTRICO

Downcomer and lower plenum experimental facility

N. Forgione, V. Baudanza, I. Angelo, D. Martelli

Report RdS/2011/109

DOWNCOMER AND LOWER PLENUM EXPERIMENTAL FACILITY

N. Forgione, V. Baudanza, I. Angelo, D. Martelli - UNIPI

Settembre 2011

Report Ricerca di Sistema Elettrico
Accordo di Programma Ministero dello Sviluppo Economico – ENEA
Area: Governo, Gestione e sviluppo del sistema elettrico nazionale
Progetto: Nuovo nucleare da fissione: collaborazioni internazionali e sviluppo competenze in materia nucleare

Responsabile Progetto: Paride Meloni, ENEA

CIRTEN

Consorzio **I**nteruniversitario per la **R**icerca **TE**cnologica **N**ucleare

UNIVERSITA' DI PISA

DIPARTIMENTO DI INGEGNERIA MECCANICA, NUCLEARE E DELLA PRODUZIONE

DOWNCOMER AND LOWER PLENUM EXPERIMENTAL FACILITY

Autori

N. Forgione

V. Baudanza

I. Angelo

D. Martelli

CERSE-UNIPI RL 1079/2011

PISA, Settembre 2011

Lavoro svolto in esecuzione della linea progettuale LP2 punto B1.b
AdP MSE - ENEA "Ricerca di Sistema Elettrico" - PAR2008-09
Progetto 1.3 – "Nuovo Nucleare da Fissione".

Abstract

This activity, performed in the frame of the research programme on “New Nuclear Fission” funded by MSE and co-ordinated by ENEA, is oriented to perform a preliminary experimental campaign on a mock-up simulating the downcomer and lower plenum of the IRIS reactor with a scaling factor of 1:5, in order to provide relevant data to study the mixing phenomena when a DVI line break accident (SBLOCA) occurs and to validate CFD codes.

In IRIS, two Direct Vessel Injection lines provide an alternative way to shutdown the reactor, by injecting borated water from two Emergency Borated Tanks directly inside the vessel. The reliable actuation of this safeguard has to be guaranteed also in case of an accidental break of a DVI line, and the boron mixing in this kind of situation has to be investigated accurately.

With this aim, a mock-up was designed at the DIMNP of Pisa University characterized by a scaling factor of 1/5 in respect to the real plant and realized at Scalbatraio laboratory.

In this first phase, the facility was set-up and used with the purpose of obtaining experimental data for CFD code qualification that can be applied to simulate the thermal-hydraulic behaviour of IRIS reactor. In particular, the experimental apparatus was accomplished without the presence of the core support plate gussets and the effects of the core support plate.

In a second step, the facility will be used to obtain experimental data in a configuration as close as possible to the IRIS downcomer and lower plenum.

This document deals in its first part with the description of the facility in its current configuration and of the instrumentation used for the preliminary test campaign.

The second part deals with the results of the CFD simulations performed by the Fluent CFD code as support of the experimental activity.

Index

Abstract ..... **ii**

Index ..... **iii**

Nomenclature ..... **iv**

1. Introduction **1**

2. Facility description **2**

2.1 Test section 2

2.2 Hydraulic circuit 6

2.3 Data acquisition system 9

2.4 Experimental test matrix 10

3. Pre-test simulations as support for experimental activity **11**

3.1 Geometrical domain 11

3.2 Approach to the numerical solution 13

3.3 Obtained results 13

4. Conclusions **25**

References **26**

Nomenclature

Roman letters

T	temperature [K]
C_B	dimensionless scalar concentration [-]
$D_{T,t}$	turbulent diffusivity coefficient [m^2/s]
$D_{C_B,t}$	turbulent diffusivity coefficient for tracer concentration [m^2/s]
t	time [s]
x_i	spatial coordinate [m]
w_i	velocity [m/s]

Greek letters

ρ	density [kg/m^3]

Abbreviations and acronyms

IRIS	International Reactor Innovative and Secure
DVI	Direct Vessel Injection
CFD	Computational Fluid Dynamics
DIMNP	Dipartimento di Ingegneria Meccanica Nucleare e della Produzione
SBLOCA	Small Break Loss Of Coolant Accident
PWR	Pressurized Water Reactor
LOCA	Loss Of Coolant Accident
HS	Heater System
DAS	Data Acquisition System
SCXI	Signal Conditioning eXtensions for Instrumentation
DAQ	Data AcQuisition
UDS	User-Defined Scalar

1. Introduction

IRIS reactor is a modular, medium sized PWR, with an integral coolant system layout [1]. Though the reactor design is based on well assessed technology, because of the effect of the integral layout and of the behavior of some innovative components, the IRIS response to LOCA accidents needs to be investigated by means of an application of the Evaluation Model Development and Assessment Process (EMDAP) to IRIS licensing process [2-3].

In many conventional pressurized water reactors, one of the most important issues is the degree of uniformity of boron concentration inside the reactor core; in fact, in certain operational or accident conditions, the presence of deborated slugs transported to the core inlet might be a risk for reactivity accidents unless a convenient level of mixing takes place [4-5]. Also in IRIS, the flow and boron mixing issues are relevant in transients in which direct vessel injection is envisaged or when overcooling due to a steam line break is taken into consideration. A specific assessment of the peculiarities of the IRIS reactor geometry, due to its large downcomer width and geometry of the lower plenum is required.

At present there are two suitable methods available for studying mixing in the downcomer and lower plenum of a pressurized nuclear reactor: downscaled model experiments and numerical simulations. The rapid development of computers and of CFD codes has made it possible to carry out simulations of large 3D problems; however, the major requirements concerning safety issues, characterising the nuclear field, recommend using special care in the validation of results provided by the CFD codes.

The present work, as part of the contribution of the University of Pisa to the IRIS project, is focused on the experimental facility description and on the thermo-hydraulic pre-tests analysis for the first experimental campaign. The aim of this analysis, performed with the Fluent code [6], was the support to the positioning of the measurement points with particular attention to the temperature sensors inside the test section.

2. Facility description

2.1 Test section

The optically transparent separate-effect facility, built at the DIMNP of Pisa University, consists of a 1:5 scaled model of downcomer and lower plenum of the IRIS reactor, designed with particular care to represent the geometrical configuration of the real plant (see red marked zone in Fig. 1). The geometrical similarity between the test section and the original reactor is respected until the core inlet, which is not reproduced in the facility and which is then excluded from the similarity.

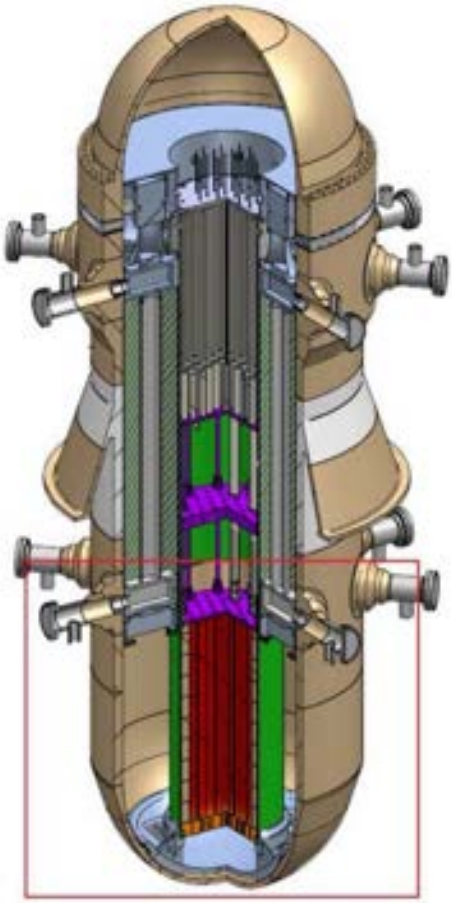

Figure 1. IRIS reactor (with the marked downcomer and the lower plenum region)

The facility is conceived to be flexible enough to make feasible both internal measurements (thermocouples and RTDs for the boron concentration, hot-wire anemometry for investigating velocity and flow detailed structures, pressure and flow rate sensors) and external flow visualization with different devices (Video Images Recorded with high speed resolution, Laser Doppler Anemometry Particle Image Velocimetry and/or Laser Induced Fluorescence).

The test section is composed of a lower hemispherical shell of Plexiglas®, having a radius of 0.623 m and representing the lower downcomer, connected to a cylindrical wall in Plexiglas®, having the same radius of the shell and a length of 0.804 m, as is represented in Fig. 2 and Fig. 3 and as is shown in from Fig. 4 to Fig. 7. An internal stainless steel cylinder having an external radius of 0.285 m and longer respect to the external cylinder in Plexiglas® completes the downcomer region. In the upper part of the facility, eight conical stainless steel pipes simulate the eight downcomer mass flow inlets coming from the eight IRIS steam generators (not reproduced in the facility). The steam generator inlets have been located at 45° angle between each other. Two stainless steel tubes, representing the two Direct Vessel Injection (DVI) lines of the IRIS reactor, are also considered with a nominal length of 0.804 m and an internal diameter of 0.0158 m. Moreover, the length of the two DVI pipes inside the downcomer can be changed to analyse the effects of their penetration inside the vessel.

The test section was designed to operate with water at a maximum temperature of 60 °C and at a maximum pressure of about 1.4 bara (just the necessary pressure to send the water that passes through the test section back to the reservoir).

The flow rate in the loop considered in this work is mainly scaled according to criterion to preserve the transit time of the coolant through the reactor model. Since the geometrical scale of the facility is 1:5, the transit time of the coolant is identical to the original reactor, when the coolant flow rate is also scaled down by 1:5.

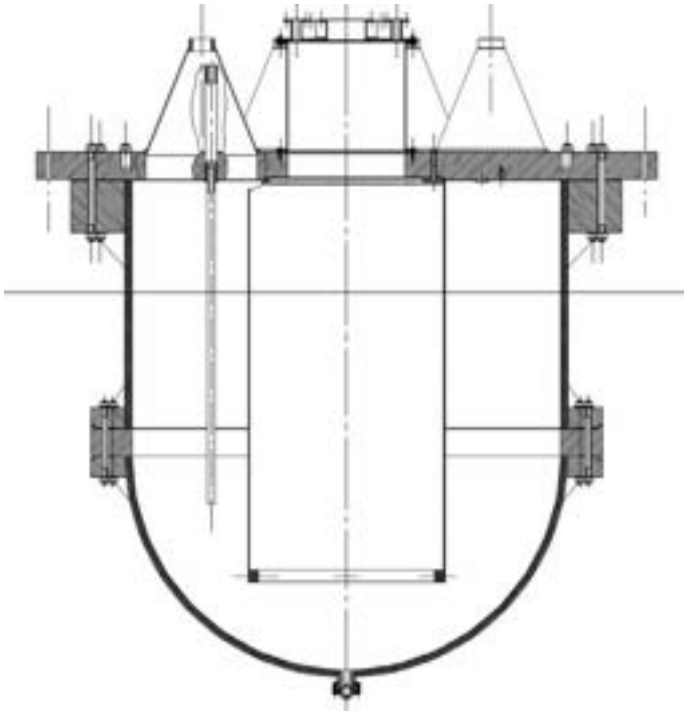

Figure 2. Test section: longitudinal cross section

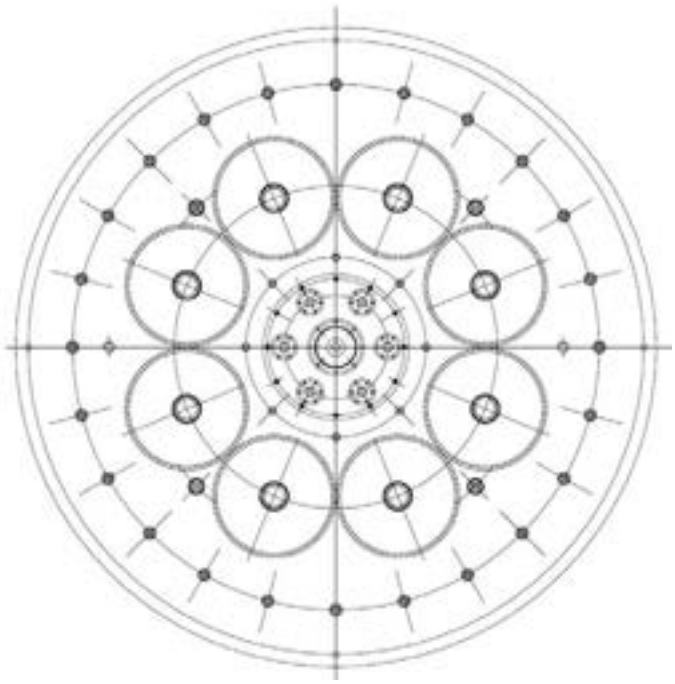

Figure 3. Upper view of the test section

Figure 4. Photos of the lateral side of test section with support frame

Figure 5. Photos of the lateral side of test section
with the vessel containing water for the two DVI pipes

Figure 6. Photos of the upper side of test section

2.2 Hydraulic circuit

The facility layout shown in Fig. 7, consists of 3 different lines:

- the primary line, in which warm water, at a maximum temperature of 50 °C, will be sent to a manifold where the flow rate will be equally divided among eight conical stainless steel pipes simulating the eight downcomer mass flow inlets coming from the IRIS steam generators;
- the secondary line, which provides the required cold water flow to the two pipes simulating the DVIs located inside the IRIS downcomer;
- the tertiary line, which controls the hot fluid temperature (the water from the primary line).

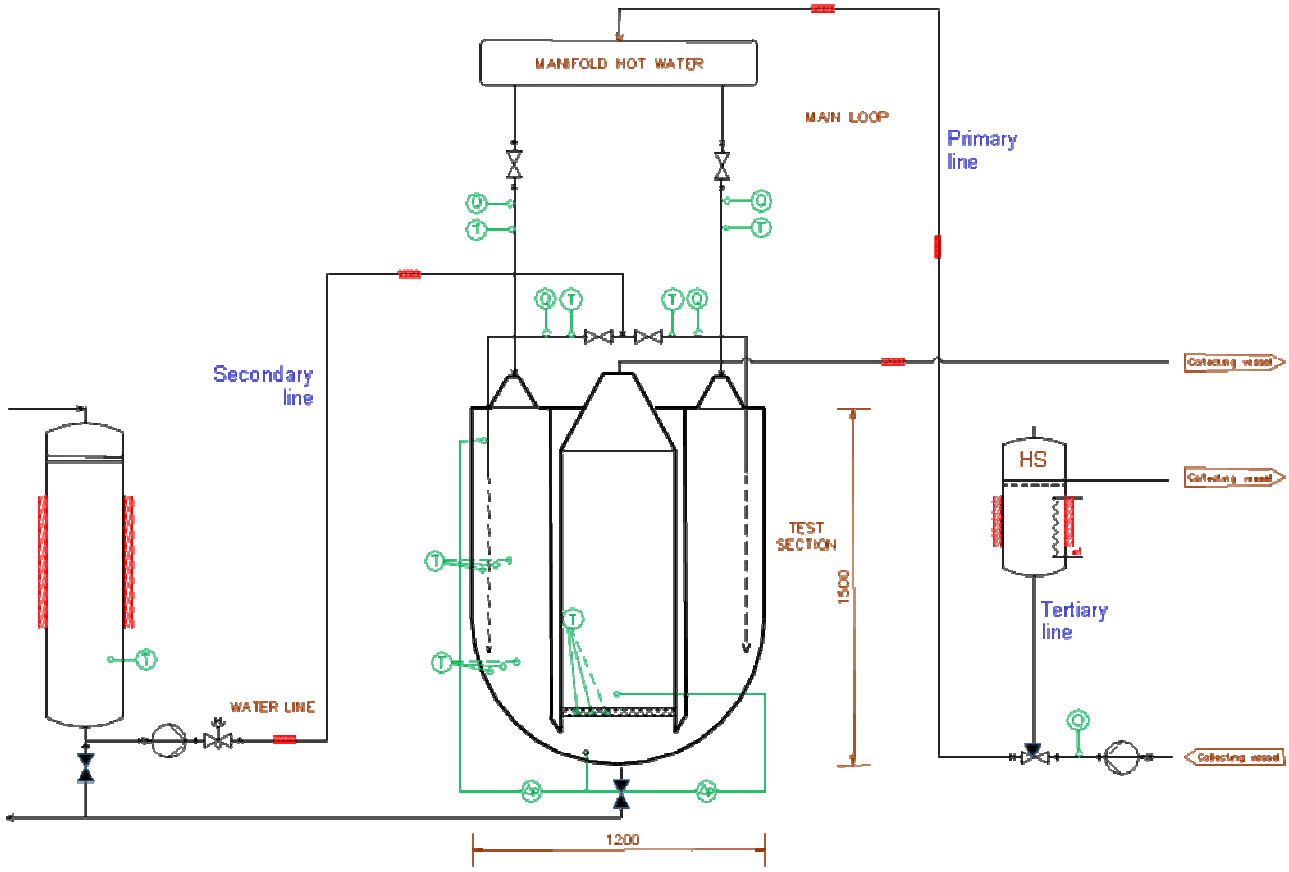

Figure 7. Layout of the facility

The warm water, passing through the primary line, comes from a large water reservoir. The temperature of about ten cubic meters of water, contained in this large reservoir, is controlled by a heater system (HS) which includes three electrical heaters (see Fig. 7 and Fig. 8). These resistance heaters have all together a maximum power of 9 kW.

Before starting the experimental test, the water contained in the large reservoir is heated at the desired temperature (less or equal to 50 °C) circulating in the tertiary loop only, acting on the three way valve shown in the right bottom side of Figure 7. After the temperature set point is reached, the warm water was circulated through the primary line into the manifold (see Fig. 9) and the heater system was bypassed. The high thermal capacity of the stored reservoir water allows tests to be performed in about one hour, without the HS activated, with a negligible reduction in water temperature inside the test section.

When a test using cold water injection (or water with a tracer inside) was foreseen the secondary line was also activated, injecting cold water from one or both the DVI pipes. In each pipe a needle valve is present (see Fig. 10) to precisely regulate the flow rate of the fluid. The flow rate in each of the two DVI pipes is measured through a differential pressure sensor connected to the Venturi device incorporated in the body of the valve.

Figure 8. Photos of the heater system

Figure 9. Photos of the manifold used to divide the inlet flow rate in eight parts (left side) and the flow rate regulator used for each of the eight inlets (right side)

Figure 10. Photos of the needle valve used to precisely regulate the flow rate of water into DVI

The measuring instrumentation available up to now includes:

- K-type thermocouples, to monitor the inlet and outlet test section fluid temperatures and fluid temperatures at different locations inside the test section, to monitor temperature differences mainly in the lower plenum and at the “core inlet section”;
- an electromagnetic flow meter, placed on the pipe coming from the reservoir and shared with the primary and terziary line;
- two differential pressure sensors used to evaluate and to control the flow in the two DVI pipes;
- a high resolution and high speed digital camera (IDT MONTION PRO Y4-S2-8-COLOR).

All the measuring instruments have been calibrated by the manufacturer (as the electromagnetic flow meter) or directly in the laboratory (as for the termocouples), to asses the uncertainty affecting every experimental data.

2.3 Data acquisition system

The Data Acquisition System (DAS), utilised for the facility, records and converts the electrical signals coming from instrumentation present in the plant. In particular, the sensors are thermocouples, differential pressure transducers and flow meters.

The DAS, showed in Fig. 11, is a network data logger based on National Instruments® devices and software and consists of the following components:

- one external SCXI (Signal Conditioning eXtensions for Instrumentation) 1001 12-Slot chassis that is used for lodging data conditioning modules to be multiplexed on the DAQ board and the DAQ itself;
- one Data Acquisition (DAQ) and Control Module SCXI-1600 of USB type on board at the chassis SCXI 1001;

- two modules of SCXI-1102B with each 32 channels (additional equipped with a SCXI-1303 front mounting terminal block) for acquiring signals up to 32 thermocouples each or other signals of tension;
- two SCXI-1125 8-Channel Programmable Isolated Input Module equipped with a SCXI-1327 front mounting terminal block for acquiring general signals of voltage with galvanic isolations.

This DAS is coupled with a personal computer with an Intel Core i5-2400 processor at 3.1 GHz.
For driving the DAQ boards and the signal conditioning modules the program LabVIEW® (Laboratory Virtual Instrument Engineering Workbench) is used. The acquisition program is set up by using "virtual instruments" available in the package.

Figure 11. The data acquisition system

2.4 Experimental test matrix

In the first experimental campaign only the mixing phenomena among water flows with different temperatures will be analyzed. In particular, the water entering from the DVI lines will be injected as cold as possible in the test section, e.g. with a temperature of 10 °C, while the water coming from the eight SG lines will be maintained at about 40-50 °C.
Starting from the results obtained in previous work [7], the three tests reported in Tab. 1 have been chosen for the first experimental campaign.

	Part	*Test I*	*Test II*	*Test III*
Flow[kg/s]	SG	5	3	1
	Single SG	0.625	0.375	0.125
	DVI 1	0.1	0.1	0.05
	DVI 2	0.1	0.1	0.05

Table 1. Matrix of tests

3. Pre-test simulations as support for experimental activity

3.1 Geometrical domain

The adopted 3D geometrical domain of the test section is shown in Fig. 12. It must be noted that, because of symmetry, only half of the test section has been considered.

As can be seen from Fig. 12, the origin of the coordinate reference system is positioned just on the symmetry plane at the vertical level in which the cylindrical part of the Plexiglas® wall is connected to the spherical bottom part.

The domain was discretized using an unstructured mesh of different sizes in order to reduce the dimension of the grids in those areas that are of most interest from a fluid-dynamics point of view (see Fig. 13). The total number of cells obtained for the domain is about 4,700,000 with smaller cell sizes in the region of DVI pipe and near the cross section representing the core inlet.

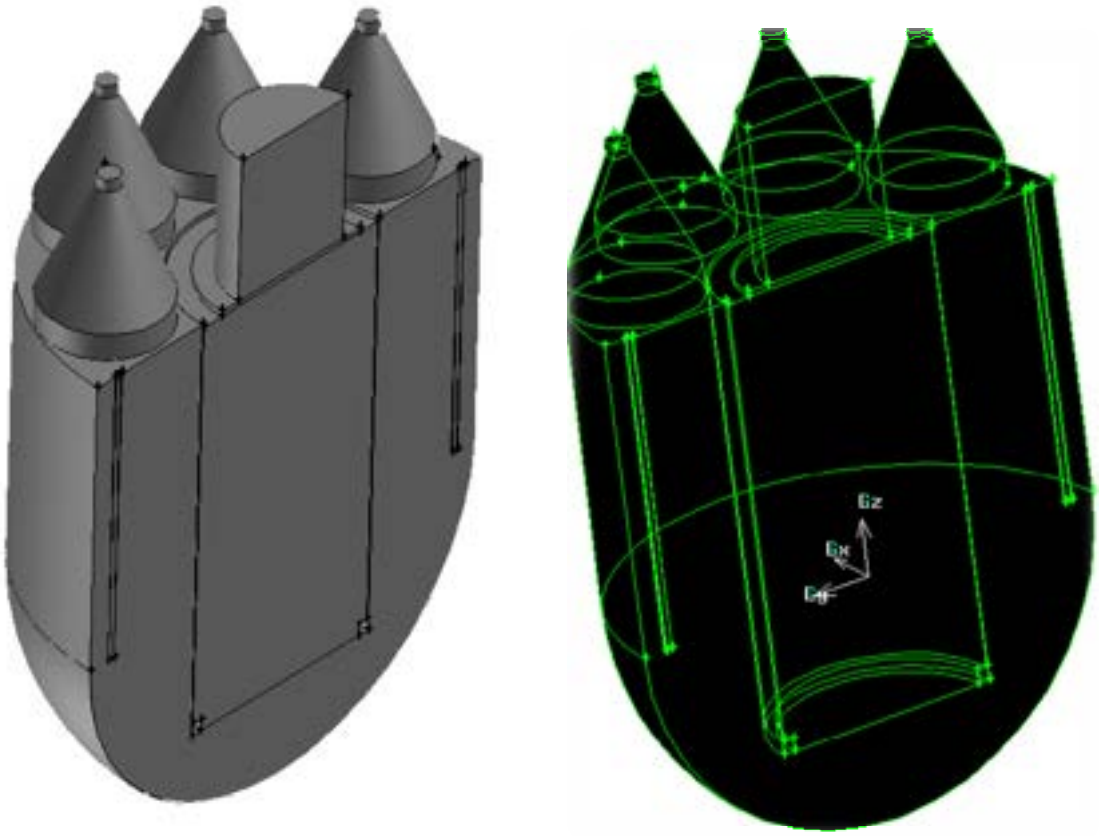

Figure 12. Geometrical domain and reference system

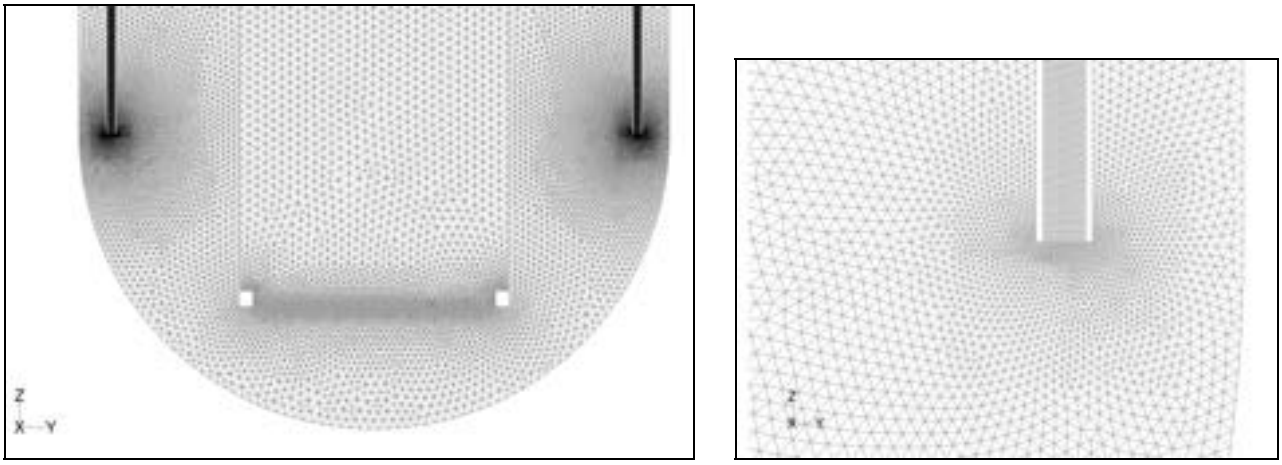

a) Symmetry plane b) Enlarged view of the mesh near the DVI's pipe

Figure 13. Spatial discretization.

3.2 Approach to the numerical solution

Since the large size of IRIS, the Reynolds number assume relatively high values in the reactor downcomer; it means that turbulent mixing is more important than molecular diffusion. The same behaviour happen in the scaled facility.

So, when a velocity field is assumed, mass and heat transfer behaviour are similar. Hence, a perturbation of boron concentration can be studied starting from the temperature field's perturbation, once buoyancy effects are negligible. As can be noted, with some simplifications, the boron concentration equation appears formally similar to the energy equation [7]:

$$\frac{\partial(\rho T)}{\partial t} + w_i \cdot \frac{\partial(\rho T)}{\partial x_i} = \frac{\partial}{\partial x_i}\left(D_{T,t} \frac{\partial(\rho T)}{\partial x_i} \right) \tag{1}$$

$$\frac{\partial(\rho C_B)}{\partial t} + w_i \cdot \frac{\partial(\rho C_B)}{\partial x_i} = \frac{\partial}{\partial x_i}\left(D_{C_B,t} \frac{\partial(\rho C_B)}{\partial x_i} \right) \tag{2}$$

where T is the fluid temperature, c_B is boron concentration, $D_{T,t}$ is the turbulent diffusivity coefficient for temperature and $D_{C_B,t}$ is the turbulent diffusivity coefficient referred to the boron concentration. Therefore, the temperature and the boron concentration profiles become similar once both the turbulent diffusivity coefficients assume values of the same order of magnitude.

Based on this hypothesis, in the facility the temperature field related to the mixing processes in the downcomer and lower plenum can be investigated instead of boron concentration distribution. As an alternative water with a tracer inside, e.g. a coloured substance, can be used to study the mixing phenomena. In this last case the conservation equation of a User-Defined Scalar (UDS) must be used in Fluent code instead of the energy balance equation.

As previously mentioned, in the first experimental campaign only the mixing between flows of water with different temperatures will be analyzed.

3.3 Obtained results

For the representation of the obtained results two planes have been chosen:

- the symmetry plane;
- the transversal section located just at the core inlet section (plane at z = - 0.360 m).

In this section only the obtained results related to *Test I* and *Test III* are presented. For each test, in order to reduce the computational effort, the fluid domain was initialized from the solution of a steady state calculation, in which the temperatures of the fluid entering from the SGs and from the DVIs ware set equal to a value of 50 °C. After reaching a steady state convergence, a transient calculation was performed, setting the water temperature entering from the DVI equal to 20 °C. The

unsteady calculations were carried out with a time step of 0.01 s for a duration of ten seconds, corresponding to the expected recording time for the available digital camera[1] (7-8 s with a resolution of about 1016x1016, 4500 fps).

All computations were performed in double precision and the "first order upwind" scheme was chosen, while turbulence was modeled using the k-ε Standard Model.

In order to investigate the mixing phenomena and to validate what established in section 3.2, further simulations were conducted, starting from the same initial condition of the previous simulation, adding a passive user defined scalar (UDS) and solving only the additional transport equation for a time simulation interval of 10 s. Results were then compared with those obtained for the temperature distribution without the passive scalar; in particular, to allow this comparison, a dimensionless temperature was introduced, defined as:

$$T^* = \frac{T_{SG,in} - T}{T_{SG,in} - T_{DVI,in}} \tag{3}$$

where $T_{SG,in}$ and $T_{DVI,in}$ are the temperatures of the water at the SG and DVI inlets.

Figure 14 shows the dimensionless temperature field after 4 s of the simulation for *Test I* (see Tab. 1). Water at a lower temperature exits the DVI mixing with water that fills the vessel at a higher temperature.

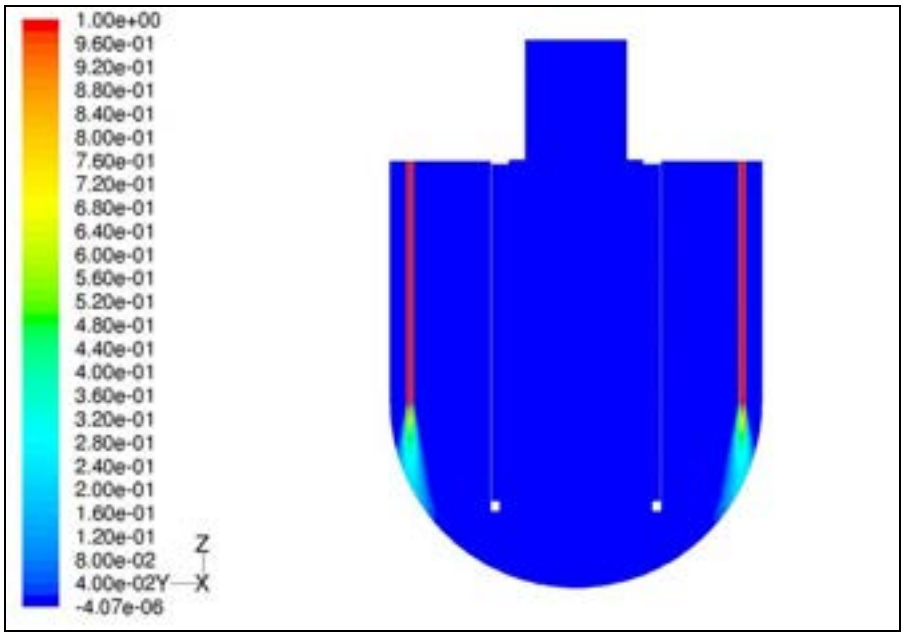

Figure 14. Dimensionless temperature distribution in the symmetry plane (t = 4 s, *Test I*).

[1] High speed camera IDT MONTIONPRO Y4-S2-8-COLOR

In Fig. 15 the distribution of the UDS at the same instant of the previous analysis and for the same test is reported.

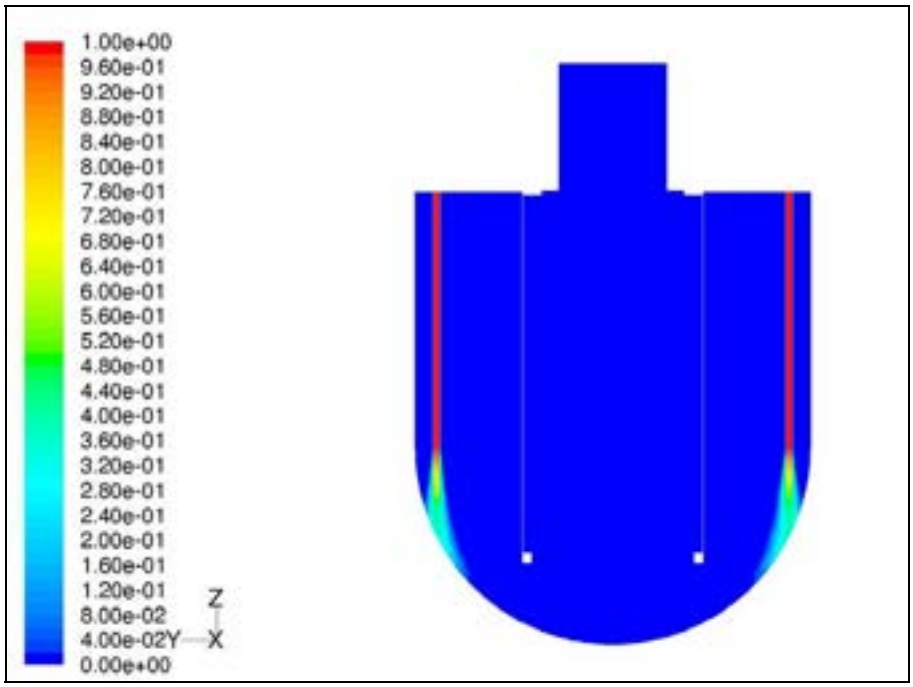

Figure 15. UDS distribution in the symmetry plane (t = 4 s *Test I*).

Good agreement in the distribution field of the dimensionless temperature and of the scalar concentration in the symmetry plane can be found comparing Fig. 14 with Fig. 15.

Figures 16 and 17 show the distribution of the dimensionless temperature and of the scalar concentration at the core inlet section (plane at z = - 0.360 m) for *Test I* and at t = 4 s. From the two contour plots we can see that the plume does not significantly reach the cross section at z = - 0.360 m, and the two distributions show negligible differences.

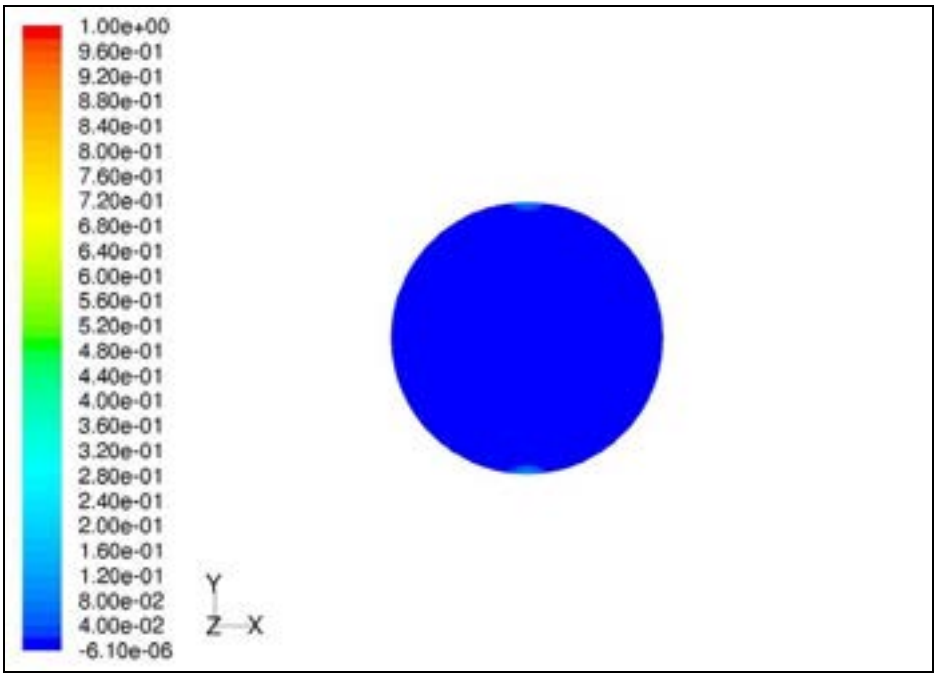

Figure 16. Dimensionless temperature distribution
at the core inlet cross section (t = 4 s, *Test I*).

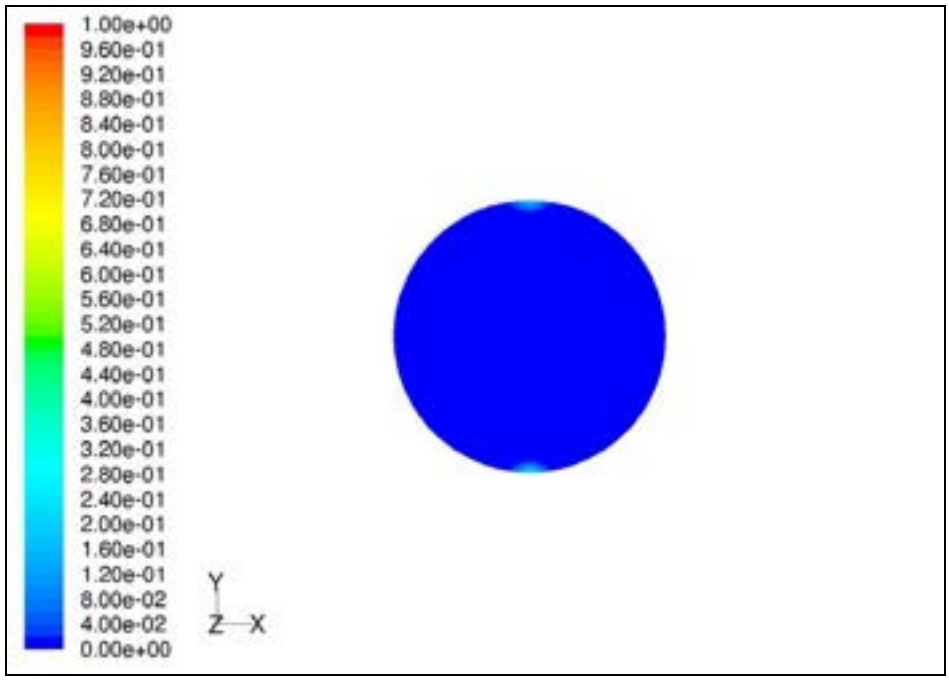

Figure 17. UDS distribution at the core inlet cross section (t = 4 s, *Test I*)

In Figs.18 and 19 are shown the dimensionless temperature and the scalar distribution at t = 10 s for *Test I* in the symmetry plane while Fig 20 and 21 show the same results at the core inlet cross section.

The foreseen distribution of dimensionless temperature agrees well with the distribution of the UDS even after 10 s of simulation (*Test I*) in the symmetry plane and cross section at the core inlet elevation, where showed differences can be considered negligible.

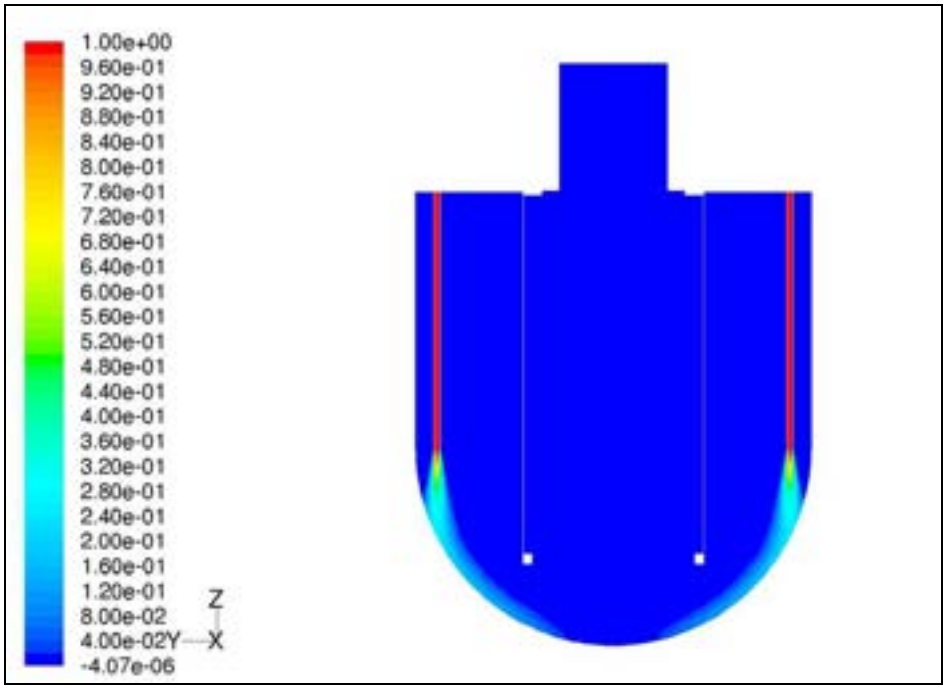

Figure 18. Dimensionless temperature distribution in the symmetry plane (t = 10 s, *Test I*).

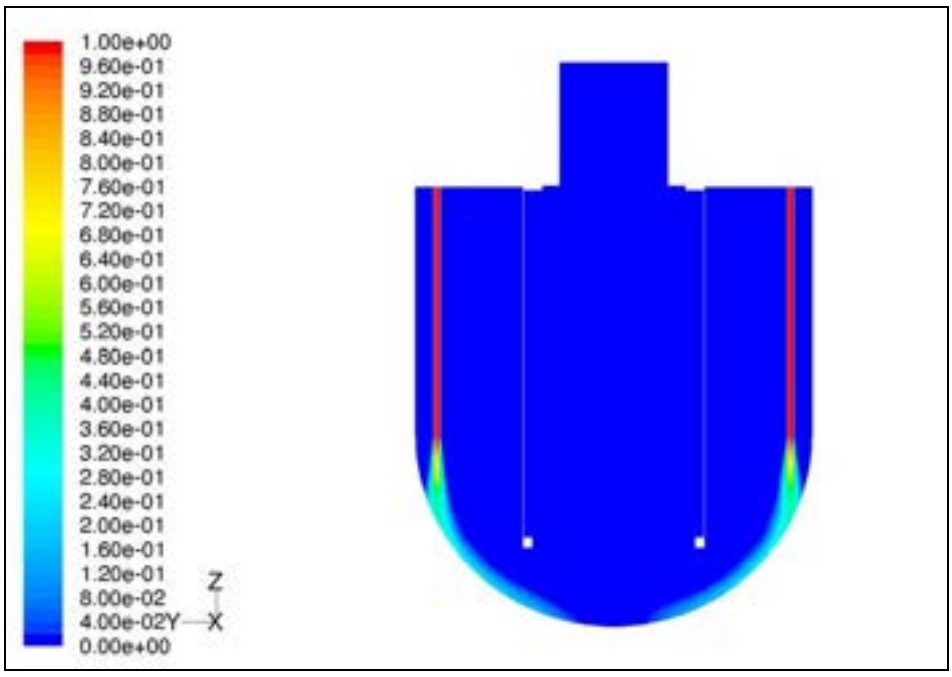

Figure 19. UDS distribution in the symmetry plane (t = 10 s, *Test I*).

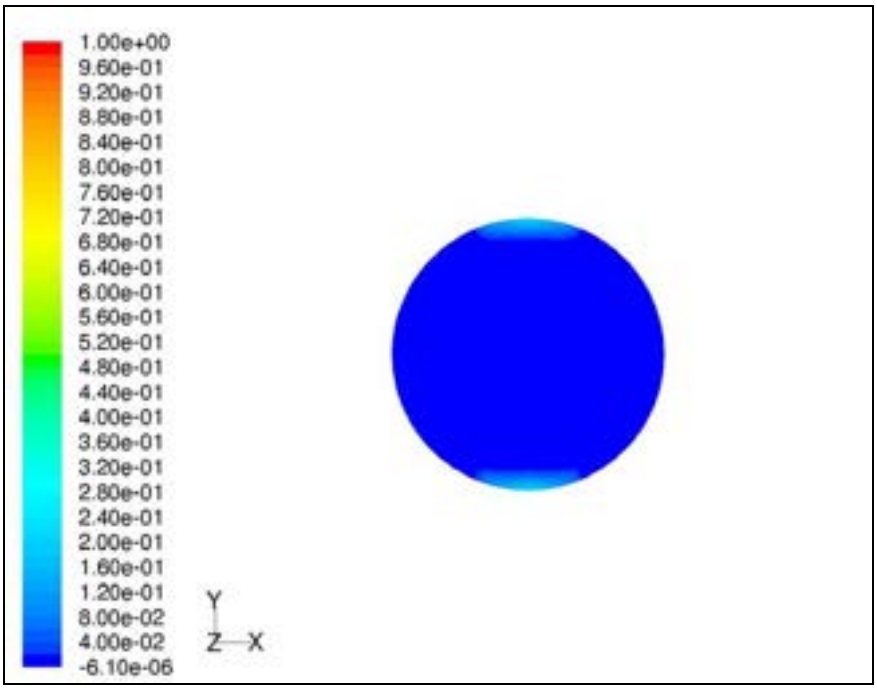

Figure 20. Dimensionless temperature distribution at the core inlet cross section (t = 10 s, *Test I*).

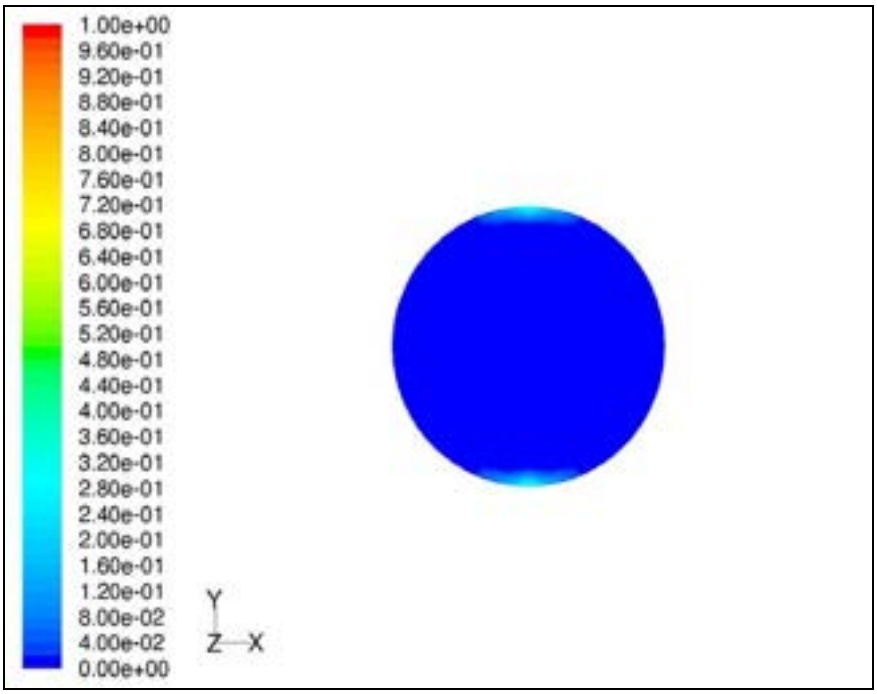

Figure 21. UDS distribution at the core inlet cross section (t = 10 s, *Test I*)

In the following section the simulation results obtained for the *Test III*, characterized by a mass flow rate in the DVI equal to 0.05 kg/s and a mass flow rate in the SG that is 1/5 of the corresponding mass flow rate of *Test I*, are presented.

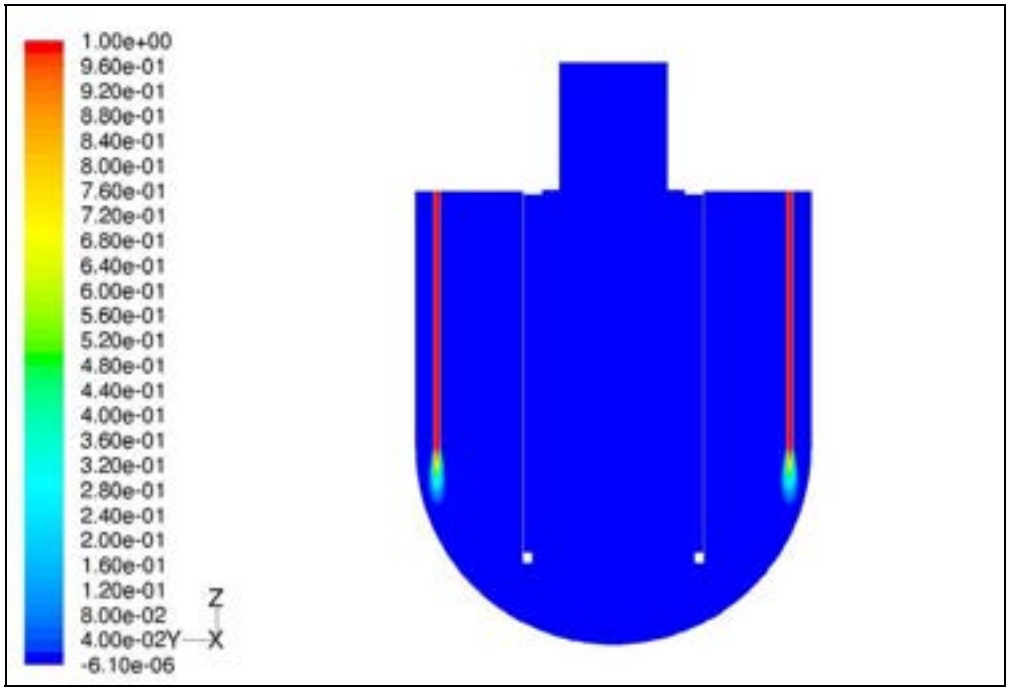

Figure 22. Dimensionless temperature distribution in the symmetry plane (t = 4 s, *Test III*).

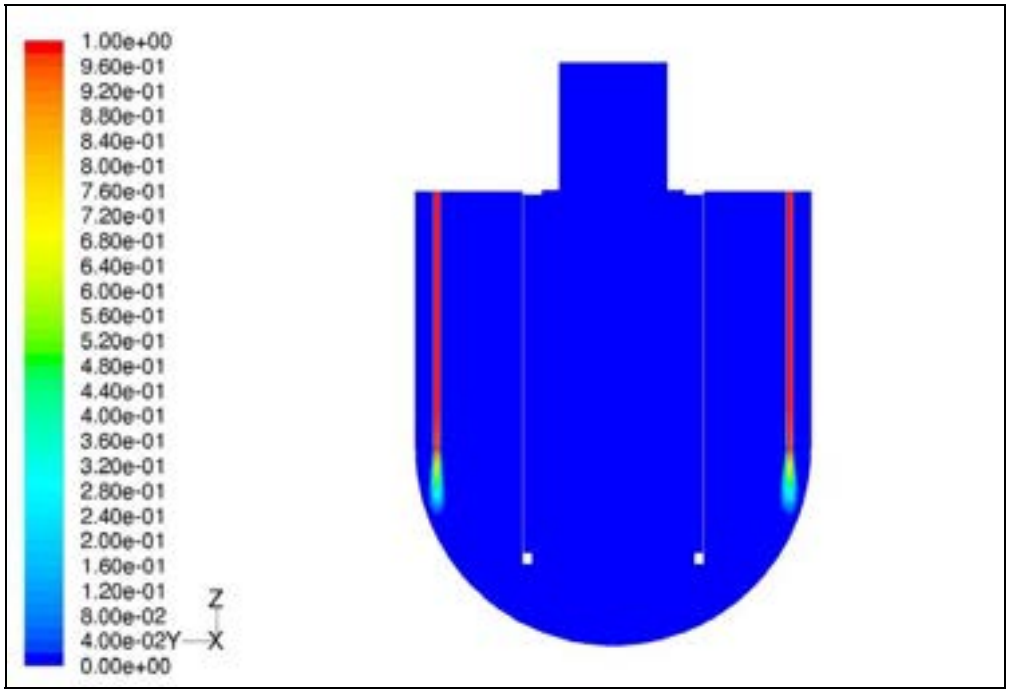

Figure 23. UDS distribution in the symmetry plane (t = 4 s, *Test III*).

Results presented in Figs. 22 and 23 show again good agreement between the two distributions; the plume at the DVI exit for the simulation involving the UDS seems to penetrate deeper into the vessel in respect to the corresponding simulation related to dimensionless temperature; this behavior, although of small entity, needs further investigation in the experimental campaign.

Because of lower mass flow rate, the flows exiting the DVI don't reach the vertical level of the inlet core section, hence the distribution in that plane for t = 4 s are not reported.

In Figs. 24 and 25 results obtained for *Test III* at t = 10 s in the symmetry plane are shown.

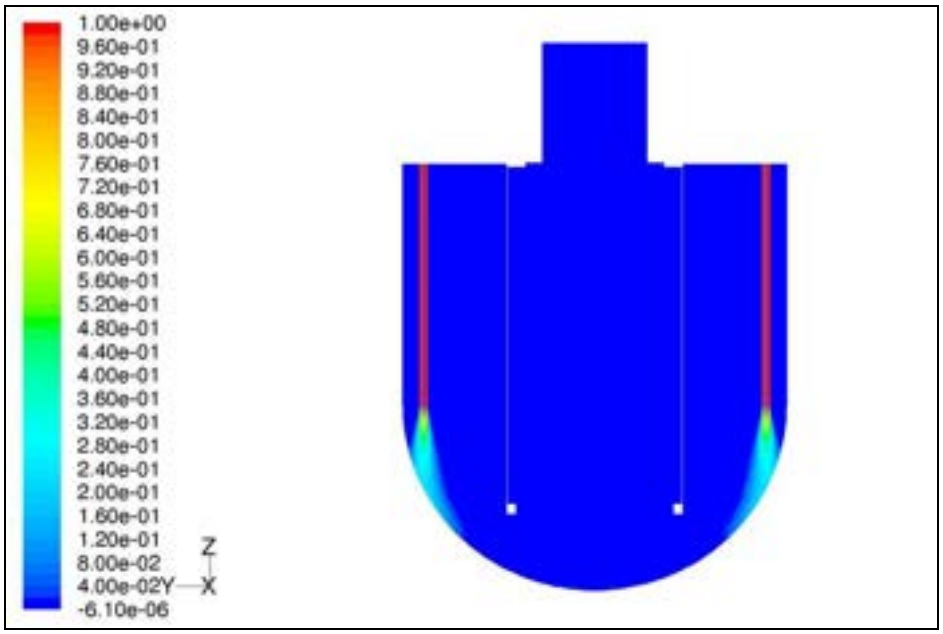

Figure 24. Dimensionless temperature distribution in the symmetry plane (t = 10 s, *Test III*).

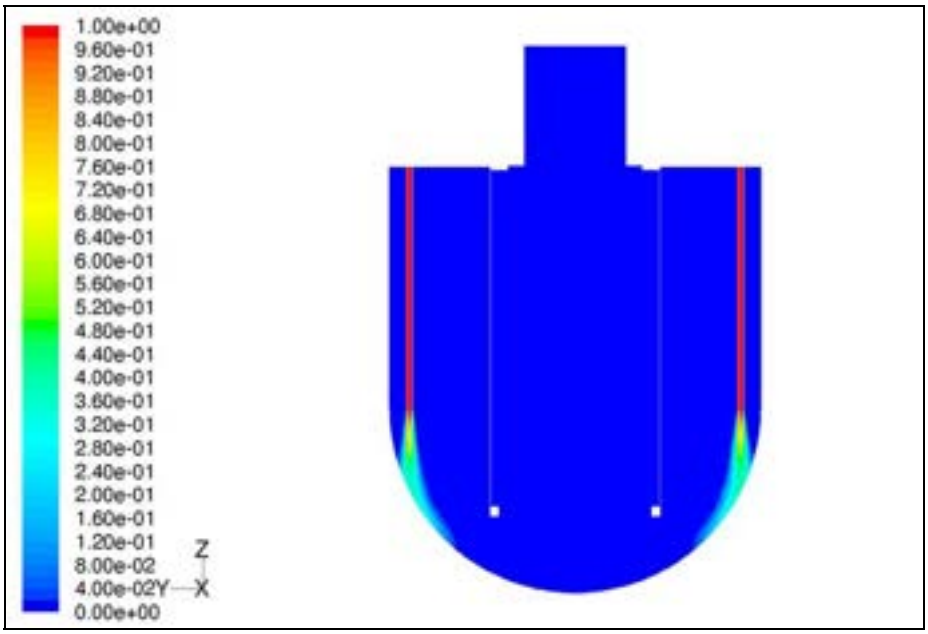

Figure 25. UDS distribution in the symmetry plane (t = 10 s *Test III*).

The obtained results show quite good agreement between the dimensionless temperature field and the UDS distribution on the symmetry plane in analogy with what was found for *Test I.*

Figures 26 and 27, related to the two distributions at the core inlet cross section, again show dimensionless temperature distribution to be very similar to the UDS distribution according to the hypothesis presented in section 3.2.

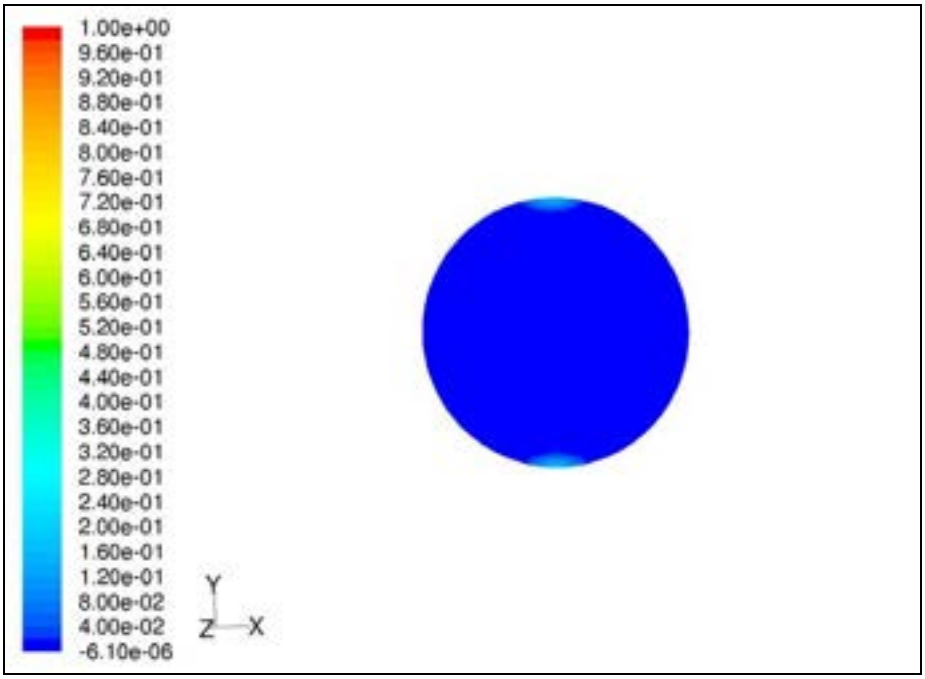

Figure 26. Dimensionless temperature distribution at the core inlet cross section (t = 10 s, *Test III*).

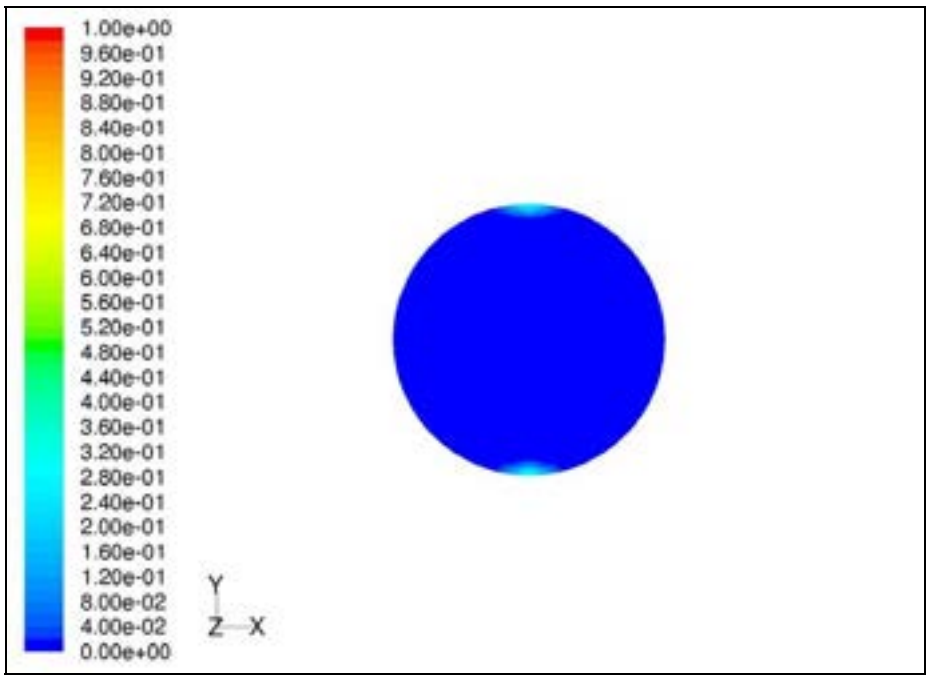

Figure 27. UDS distribution at the core inlet cross section (t = 10 s, *Test III*)

Comparing results obtained for *Test I* with those related to *Test III*, we found in the latter test a lower extension of the cold fluid exiting from the DVI according with the lower mass flow rate imposed at the entrance (see Table1).

Figures 28 and 29 show the velocity vector distribution in the region close to the exit of the DVI for *Test I* and *Test III*, respectively. The velocity magnitude reach a maximum value of about 0.63 m/s (see Fig. 28) for an imposed mass flow rate of about 0.1 kg/s (*Test I*), while the maximum velocity reached about 0.324 m/s (see Fig. 29) for an imposed mass flow rate of 0.05 kg/s (*Test III*).

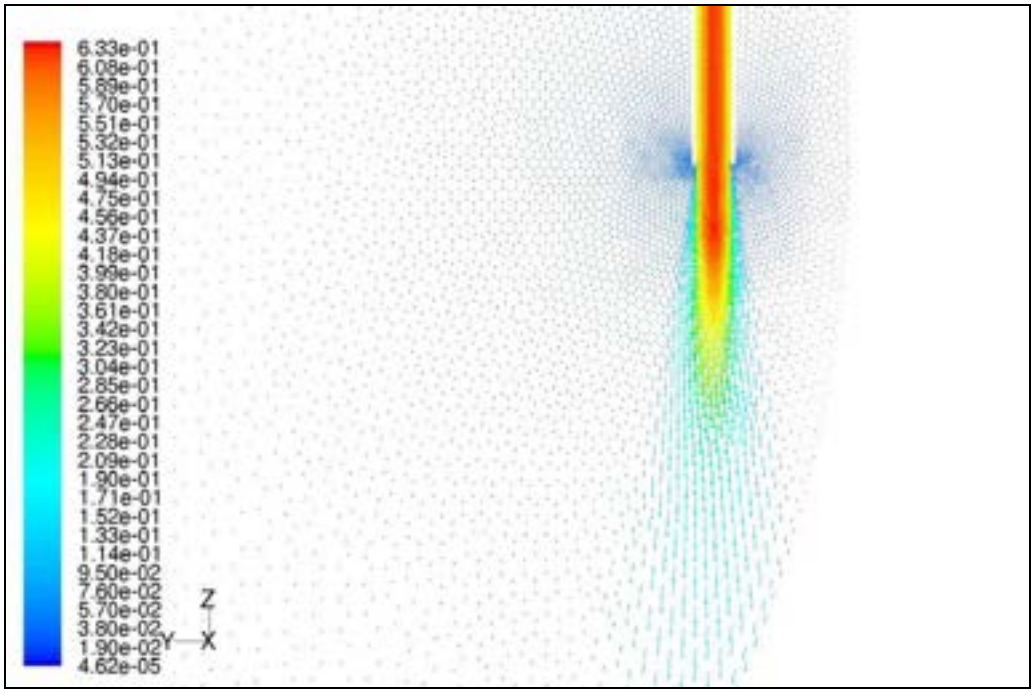

Figure 28. Vector field velocity enlargement at the DVI output (*Test I*)

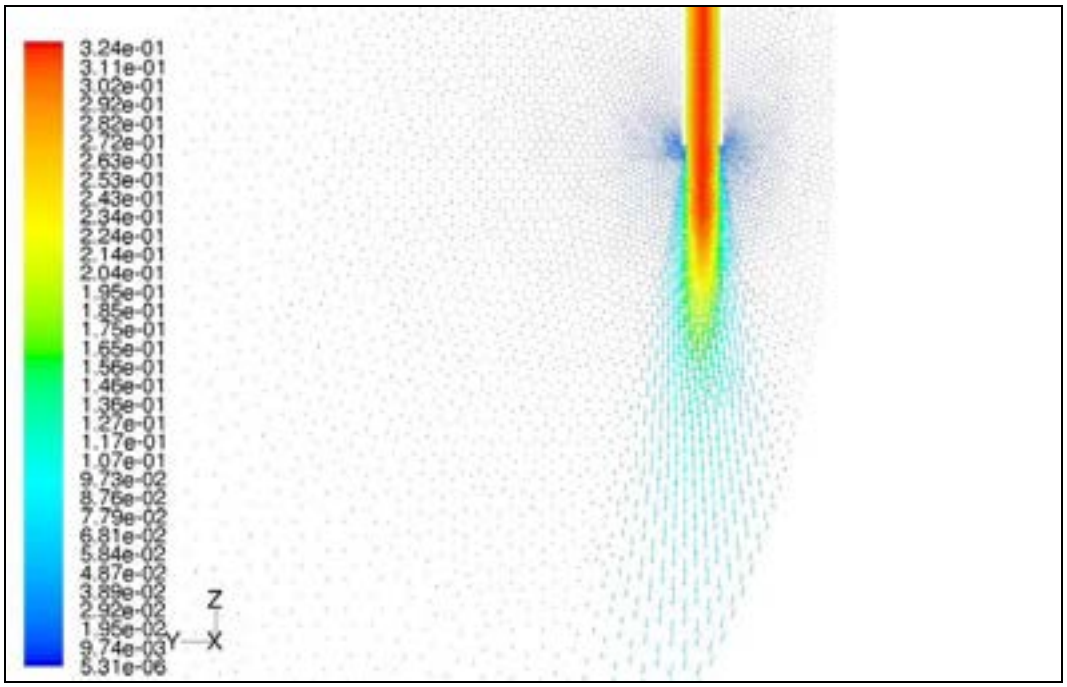

Figure 29. Vector field velocity enlargement at the DVI output (*Test III*)

Considering that the digital camera records 7-8 s with the requested resolution and that we are interested in the analysis of mixing inside the vessel, the time needed for the tracer to reach a concentration of about 100% at the exit of the DVI is investigated for both *Test I* and *Test III* monitoring the concentration in a point located at 0.05 m behind the exit of the DVI along its axis. The obtained results are reported in Fig. 30 where it is possible to see, as for *Test I*, that the tracer starts to flow inside the vessel after about 1 s from the beginning of simulation, while for *Test III* this time shift was about 2.1 s.

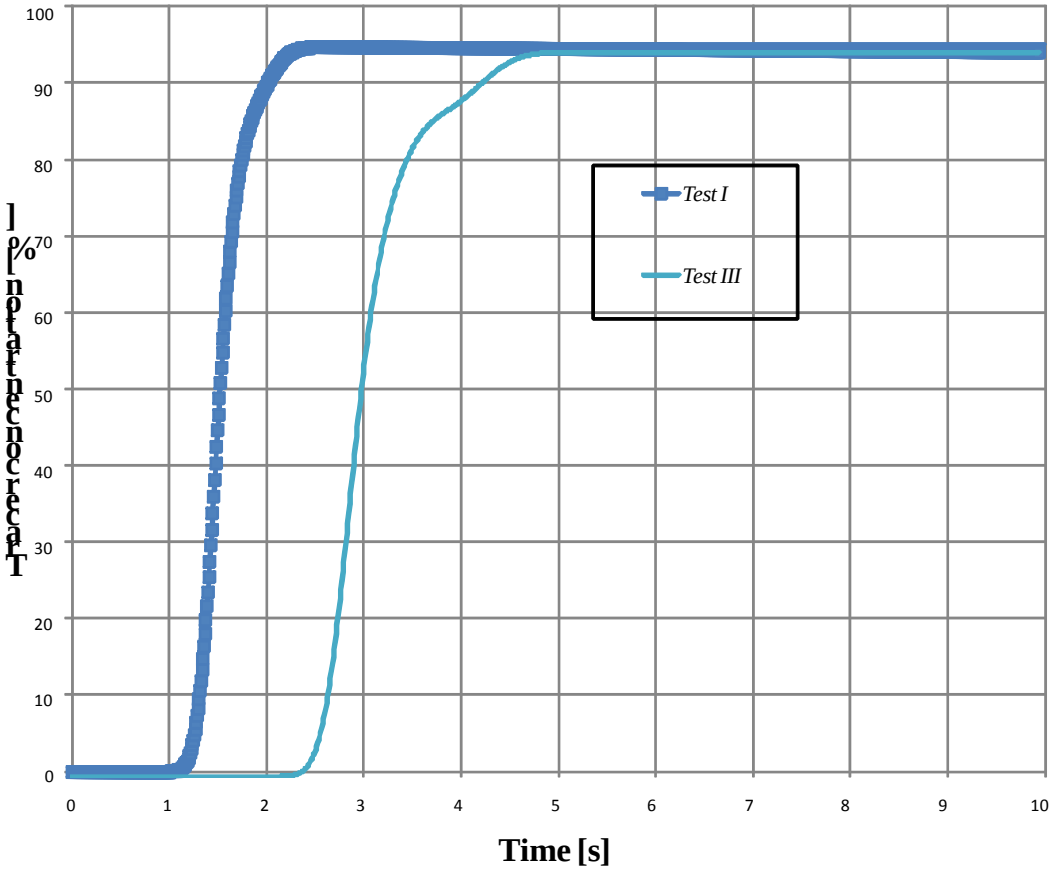

Figure 30: Tracer concentration at z =-0.05 m along the DVI axis.

4. Conclusions

A new experimental facility was built at the DIMNP of the Pisa University having a detailed study of the flow field and of the mixing phenomena in a relevant configuration for the downcomer and the lower plenum of the IRIS reactor as a main purpose. The experimental facility was designed to be flexible enough to implement the residence time-preserving criterion or velocity-preserving conditions and to add components later, in order to simulate in detail the water flow in IRIS reactor.

The current configuration of the test section was set-up with the purpose of obtaining accurate experimental data for CFD codes qualification, as Fluent commercial code. In particular, for the first experimental campaign three tests are considered more meaningful for code qualification; the differences among these tests consist mainly in the different mass flow rate of warm water injected in the eight conical stainless steel pipes. In all the tests both the DVI pipes are activated with the purpose of studying the temperature field inside the downcomer and lower plenum, relating to the mixing processes of the cold water coming from them with the warm water flowing from the steam generator inlets.

Pre-test calculations were performed for two experiments of the foreseen test matrix, with the CFD Fluent code, in order to identify relevant phenomena in the downcomer and lower plenum, like vortex formation, recirculation regions and mixing characteristics, thus setting up the appropriate instrumentation and locate them in more significant positions.

The comparison between the calculated distribution fields of dimensionless temperature and of the user defined scalar (representing a coloured substance or the boric acid concentration) confirmed the hypothesis that, in the analysed conditions, molecular diffusion can be neglected in respect to the turbulent diffusion. Therefore, in the facility the temperature field related to the mixing processes in the downcomer and lower plenum can be investigated instead of boron concentration distribution.

References

1 Mario D. Carelli, L.E. Conway, L. Oriani, B. Petrovi´c, C.V. Lombardi, M.E. Ricotti, A.C.O. Barroso, J.M. Collado, L. Cinotti, N.E. Todreas, D. Grgi´c, M.M. Moraes, R.D. Boroughs, H. Ninokata, D.T. Ingersoll, F. Oriolo, "The design and safety features of the IRIS reactor", *Nuclear Engineering and Design*, 230, pp. 151-167, 2004.

2. Regulatory Guide 1.203, "Transient and Accident Analysis Methods," USNRC, December 2005.
3. Dzodzo M. B., "EMDAP- Method for scaling Analysis", Westinghouse Electric Company - Science and technology Department, *3D S.UN.COP 2007: 6th seminar College Station*, Texas, USA, 22 January-9 February, 2007.
4. Kiger K.T., Gavelli F., "Boron mixing in complex geometries: flow structure details", *Nuclear Engineering and Design*, 208, pp. 67–85, 2001.
5. Rohde U., Kliem S., Höhne T., Karlsson R., Hemström B., Lillington J., Toppila T., Elter J., Bezrukov Y., "Fluid mixing and flow distribution in the reactor circuit, measurement data base", *Nuclear Engineering and Design*, 235, pp. 421–443, 2005.
6. Fluent 6.3.26 User's Guide Documentation, Lebanon, USA, 2006.
7. Carnevali A., Forgione N., Galgani G., Oriolo F., "CFD Analysis in Support to the Experimental Activity on the Mixing Processes in the Downcomer and Lower Plenum of IRIS Reactor", CIRTEN-UNIPI RL 1077/2010, Pisa, agosto 2010.